RESEARCH

Laser welding in e-mobility: process characterization and monitoring

Caterina Angeloni[1] · Michele Francioso[1] · Erica Liverani[1] · Alessandro Ascari[1] · Alessandro Fortunato[1] · Luca Tomesani[1]

© The Author(s) 2023

Abstract

The global automotive industry is shifting to e-mobility, where the main challenge is addressed to battery's mass-production. To keep up with the market demand, high speed production rates and quality products must be accomplished. Since laser welding of dissimilar thins sheets has earned rising demand for battery electrodes connections, a defect-free welding process has to be performed on behalf of a closed-loop monitoring system that updates corrective and/or preventive actions in order to obtain a reliable, "zero waste, zero stop" process. However, nowadays photodiode systems do not allow real-time modification of the parameters, they only tell, at the end of the process, if any signal has gone out of threshold. The objective of this paper is to find correlations between the data collected by the monitoring system with the typical process characteristics of laser welding. Materials investigated are pure copper 300 μm and aluminum 400 μm, processed by means of different sources, length tracks, wavelengths and scanning heads. In this contribution, a Precitec system has been implemented as a possible economical and industrial-oriented solution.

The experimental data was analyzed offline and the relationships between technological and signals outputs were evaluated by means of statistical analysis with MATLAB for both Al-Cu and Cu-Al configuration. Findings plotted stable signals if high speeds were set. Results further suggested the power to be the most influent variable for the closed-loop monitoring system and the dependance on the first material irradiated and the laser source used to define the threshold value for the control of the welding process.

✉ Caterina Angeloni
caterina.angeloni2@unibo.it

[1] Department of Industrial Engineering (DIN), University of Bologna, Viale del Risorgimento 2, 40136 Bologna, Italy

Introduction

Nowadays it is well known that the future of Mobility is Electric, ranking first among the solutions in the automotive field to address the reduction of emissions into the environment. European Parliament states that by 2035, all new cars manufactured for the EU market should produce *zero-emissions*[1]. However, switching to electric mobility represents for many companies a fundamental revamp of production technology. The electrical energy storage system is the most critical feature since the battery is the most expensive and the heaviest component inside the electric vehicle. Many companies operating in this field are adopting lithium-ion batteries because of their advantages in terms of high energy density, making them easier and faster to charge and long-lasting. There are three battery geometries for automotive applications: cylindrical, prismatic and pouch. These geometries are assembled into modules which are put together into a battery pack. The number of modules and, consequently, batteries are chosen depending on the power/energy that must be supplied by the vehicle[2].The pouch cells that contain the battery are equipped with two contact tabs made of copper and aluminum for anode and cathode. When more cells are mounted in a battery pack, electrical connections are needed between these contact tabs in order to get a serial connection of the cells[3]. Welding processes are suitable to create such contacts characterized by high strength and low electrical resistance.

In this context, laser is becoming a fundamental tool thanks to its flexibility in terms of automation and control, therefore can be easily inserted into industrial production. In particular laser-welding is widespread thanks to its production speeds and accuracy, which are the highest in the entire panorama of technologies. Automated production itself calls for a high number of welds and a wide range of differences in terms of materials, thickness and welding units involved in the process.

Lap- or butt-joint welding of dissimilar highly reflective metals, such as aluminum and copper, has been widely investigated, as shown by Katayama et al.[4]. The latter discern thoroughly more than one-hundred papers on laser welding of thin metal sheets. It is therefore well known how to weld a proper seam in hybrid configurations. The challenge today is when it comes to high production rates and high demand of quality required by a zero-defect process. Industrial production speeds can reach up to 5–10 batteries/sec and the assembly of a single battery pack can contain up to 20,000 welds [5]. It is estimated that each Gigafactory produces 6% circa of defected cells and battery modules [6]. Since most of the materials (electrodes, cell separators, electrolytes) are not fully recyclable and the whole disposal process is pricy, the quality target of the process has been set to 99.7%[6]. This highlights the central role of a monitoring system that gathers information from the process, improving the understanding of the detecting phenomena. It uses the collected data to create quality control methods and adaptive, closed loop control of the process[7]. Hence, as the number of destructive samples inspections are minimized, the implementation of a monitoring system can be seen as a product certification.

A lot of studies of online quality control have been carried out aiming at reducing or eliminating product quality defects and process errors. Nowadays

monitoring systems range from simple systems using single sensors to more sophisticated systems which utilize a great deal of sensors and detection methods, as shown by Katayama et al.[8] and Cai et al.[9]. The latter reviewed three-hundred-ish papers describing the typical sensors used for laser welding and adaptive control: it ranges from photodiodes, visual sensor, spectrometer, acoustical sensor, pyrometer, plasma charge sensor to the application of artificial intelligence algorithms. It states that, to date, it is consolidated that the geometry of the melt pool exerts a major influence on the weld. That's why researchers are now assessing imaging as a tool in monitoring and predicting weld's quality. Moreover, machine learning (ML) models have been exploited since they are able to learn the error between the predicted value and the real value. Especially, deep learning is the present research highlight [9].

To date, a wide range of ML algorithms have been applied for the classification of selected defects. For example, Schimdt et al. [10] found that FRESH algorithm well classifies a spatter and a no spatter weld based on photodiode data gathered in-process. Lee et al. [11] demonstrated the feasibility and applicability of neural network classification to classify Al/Cu laser weld penetration as unsatisfactory, transient, or good in photodiode signals.

Blug et al. implemented a closed-loop system based on the observation of the penetration depth of keyhole welding processes on aluminum foils. A stochastic approach was implemented for the relation between laser power and the probability to detect full penetration hole. A CNN based system called Q-eye developed by Anafocus was used to execute the algorithms for the detection of the full penetration hole. The optics units were mounted to the coaxial process window of the welding head in order to create the thermal image in the spectral range of 820 to 980 nm. A 20 m cable connects the camera with the CNN control unit, which contains the interface to the laser control unit on the one hand and the PC on the other hand. The latter runs the control software which functions as the user interface. The results show that the standard deviation of the laser power was in the order of 2% [12].

Ascari et al. [13] proposed a method to ascertain the laser weld depth of battery connector tabs (Al e Cu thin foils) using *optical coherence tomography* (OCT) equipment. An adjustable ring mode (ARM) laser integrating OCT technology with two beams was exploited: one pointing at the bottom of the keyhole and the other one referring at the sample's surface. They used the "Keyhole Mapping" approach, which identifies the optimum positioning of the OCT measuring ray. Considerations on both the measurement's accuracy and the keyhole stability were made. It was demonstrated that ARM laser returns a more stable process as it reduced the fluctuations of the opening of the keyhole and it improved the measurement accuracy by the 50%.

Recently, part of the research focuses on the implementation of *deep learning* and *digital twin algorithms*. Good results were achieved by Franciosa et al. studies [14]. It presents a digital twin framework for assembly systems combining sensors with deep learning and CAE simulations. This study developed a closed-loop in-process control using a fully digital developed remote welding process for aluminum doors for e-mobility applications. It can identify the main causes of quality defects and suggest corrective actions for automatic defects mitigation.

The above studies are based mostly on deep-learning methods that can achieve only one prediction task. As laser welding is a complex phenomenon that is influenced by multiple parameters, multiple tasks have to be accomplished, as the work of Kim et al. shows [15]. Another study carried out by Franciosa et al. [16] developed a method for closed-loop in-process quality control in battery assembly lines. It is based on a holistic approach exploiting the potential use of *light-based technology*. The authors exploit both in and off-process methodologies to monitor the process: SEM scanning (off-process) to correlate grain structure with the material strength status, CT scanning (off-process), Optical measure (off-process) to evaluate weld penetration depth and weld interface width, Laser radiation (in-process) to measure weld depth penetration through OCT technology, thermal radiation (in-process) inspected with a IR camera. The closed-loop system is based on the development of a low fidelity artificial intelligence model, which identifies critical patterns in data flows that are then improved by implementing Multiphysics simulations.

Seibold et al. [17] realized a process control by real-time pulse shaping where the power is adjusted in each pulse. Al-Cu thin foils were welded, and it was found out that the steps of the welding process can be captured and recognized by using photodiodes with band-pass filters.

Currently, there is little research on effective closed-loop industrial solution that can be implemented in an industrial environment: most of the technologies cited previously involved an equipment that is complicated, bulky and pricy, making them suitable just for experimental studies. Only a simple and flexible monitoring system can cope with rapid product variety in terms of materials and geometries that can be processed.

In this direction, this paper considers a low-level system which includes photodiodes sensors PD (Laser Welding Monitor LWM 4.0). A *low-level* system is a *ready to use* industrial system: a PD can be defined as a commercial sensor that can perform direct measurements and be easily integrated into different setups and detect different wavelengths ranges. This kind of monitoring systems for mass production integrated in the production line nowadays do not allow a real-time modification of the process parameters, they only state, at the end of the process, if any signal values have gone out of range, which has been established previously during high-quality welding.

In literature it is described which parameters have the major influence on the process quality in laser welding but there is a consistent lack of information on the correlation between physical phenomena and sensor response. Big Consistently, the aim of this paper is to investigate the in-process signals measured by photodiodes and the level of correlation between the three signals in order to improve our understanding of the feedback they provide, both individually and together. To accomplish this, experimental tests on Cu and Al thin plate were performed by varying laser power, welding speed and the length of the trace while monitoring the signals of the three photodiodes. The experimental data was evaluated offline and analyzed to evaluate the relationships between technological and signals outputs.

Table 1 Physical properties of aluminum and copper [19]

	Copper	Aluminum
Density [g/cm^3]	8.9	2.71
Melting temperature [°C]	1083	660
Thermal conductivity [W/ (m ·K)]	390	226
Thermal expansion coefficient [°C^{-1}]	$17 \cdot 10^{-6}$	$24 \cdot 10^{-6}$
Specific heat capacity [J/ (kg K)]	385	880

Fig. 1 Laser system set-up. Galvo head, Precitec monitoring system and clamping device position are highlight with white circles
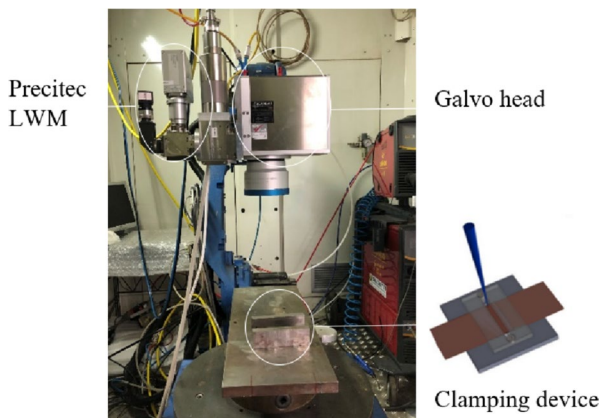
Materials and Method

The welding experiments were carried out using pure copper (Cu > 99.6%, 0.3 mm thick), coated with a thin nickel layer in order to improve optical absorptivity of the laser radiation [18] and to avoid surface oxidation, and commercially pure aluminum AA1060 (99.4% Al, 0.25% Si e 0.35% Fe, 0.4 mm thick). The physical properties of both materials are shown in Table 1. Welds were performed on samples in a lap-joint configuration. For all the tested process parameters, both Al-Cu (aluminum on top) and Cu-Al (copper on top) configurations were examined in order to understand the importance of laser absorption and melt pool dynamics during re-solidification. For the purpose of keeping the adhesion between the two sheets during the process, a clamping device was used. As Fig. 1 shows, the clamp consists of two plates in which the two metal sheets are pressed together by means of two screws positioned at the two ends of the slot. The upper smaller plate consists of a slot which facilitates in accommodating the laser beam during laser welding and both ends of the same plate are screwed to the lower plate to hold the sheets together.

Methodology

Laser welding equipment and Optical Setup

Two near-infrared fiber laser sources were selected for the experiments. A single mode and a multimode laser source delivered by feeding fiber with core diameter respectively of 49 and 68 μm were used in a continuous (CW) mode for weld tests. The multimode source was a nLight Alta 3KW, while the single mode source was a nLight CFL-1200. The characteristics of both laser sources and optical systems are shown in Table 2. The motions of the laser beam to perform linear weldings were achieved by a galvo scanning head for both configurations to maximize the laser speed, while the initial displacement of each weld was carried out by (ROBOT Motoman HP-20 six axes). The Precitec monitoring system, fully described in the following 'Process Monitoring' section, was mounted on the scanning head, as Fig. 1 shows.

The full experimental campaign is described in Table 2. After defining a feasibility window, the effects of power and welding speed on the weld bead geometry were assessed. Only the first test was conducted with the multimode laser source, while the single mode laser source was implemented in the second and third trial. Each of the three tests includes nine weld beads and was repeated twice, for a total of 54 weldings for each configuration. If a signal value was found to be very far from repetition, a third test would have been carried out, which was then not necessary. The results reported in the Result section are the average of the two tests. All experiments were performed without shielding gas and without filler wire for reducing external influences on monitoring signals. In order to avoid surface contamination, samples' surface was cleaned before welding.

The two different F-Theta lenses installed in the galvo scan head lead to different spot dimensions. A 19% larger spot results from multimode laser configuration, therefore higher laser power and slower speeds are needed to get roughly the same energy density, defined as the product between power density and interaction time [J/cm3]. See Table 1.

Table 2 Multimode and Single mode Laser source properties

Laser source			Optical Path		
Specific	Value		Specific	Value	
	Multi mode	Single mode		Multi mode	Single mode
Beam's wavelength [nm]	1064	1064	Collimation length [mm]	120	120
Operative Method	CW	CW	Focal length galvo [mm]	163	420
Max Laser Power [W]	3000	1200	Fiber diameter [μm]	50	14
BPP [mm·mrad]	2	0.4	spot [μm]	68	49

In the third test, only the length of the linear weld track was increased from 48 to 100 mm to discern the influence the influence of weld-path on weld-bead geometry and measured signals. A comparison was then made with the previous tests.

At the end of the experimental campaign, the welds were sectioned in the middle of the bead and were prepared for metallurgical analysis by using standard criteria for sample preparation. Cross sections of the weld joints were mounted in resin and then polished with SiC paper grit from 800 to 2500 followed by 1 μm alumina suspension. The metallurgical specimens were etched with Keller's reagent (1 ml HF, 1.5 ml HCL, 2.5 ml HNO3 and 95 ml H2O) with an etching time of 20 s for preliminary observation. Micrographs and weld bead measurements were taken with a ZEISS Axio Vert.AlM for a visual correspondence of the results obtained.

Process monitoring

The Precitec monitoring system used (LWM 4.0; Precitec GmbH, Germany) assures non-destructive online control in real time. As Fig. 1 shows, the system is mounted on the camera flange located on the laser head. Hence, the internal optical path in the welding head is used, meaning that the sensors are always coaxially aligned to the welding spot and preserved from contamination. The system contains 3 photodiodes which detect the luminous intensity of three radiations emitted over three wavelength ranges. These detectors collect plasma signal (PS), temperature signal (TS) and back-reflection signal (BS) at a maximum sampling rate of 1 kHz.

- The plasma sensor documents the UV light (<400 nm) and luminous radiation VIS (450 nm – 580 nm) from the plasma plume by recording and analyzing the amplitude. The plasma control variable itself indicates the amount of metal vapor ionized during the keyhole formation process [20].
- Back-reflection is that fraction of the laser beam which is not absorbed by the material and therefore emits at the same wavelength as the laser. The sensor record optical emission with wavelength within the following range:1020 nm – 1090 nm). It is consolidated that the BS is directly correlated with the keyhole geometry, thus providing information about the penetration depth [21].
- The temperature detector captures radiation in the near infrared NIR (1100 nm – 1800 nm) and gives information on the thermal condition of the irradiated surface. Hence, the TS enables the identification of lack of fusion.

Both hardware and software gains were set to clamp the signals in the range [0,10] V.

The system stores all the process signals in the SQL-Database, which is used to manage the Measurements and Configurations. The Control Module happens to be the core connection between the database, one or more View modules and possible external units connected by the customer. The View Module in the software guarantees a visualization of the processed signals. All the measurements were then selected and exported as.txt files, which were then given as an input for a short MATLAB script whose purpose was to graph the data and perform statistical

analyses. The statistical features extracted from each raw signal of a weld are the mean value (T_m, P_m, B_m) and the standard deviation (T_std, P_std, B_std). The average between the two repetitions is then stored in one datapoint. As a result, every point in the dataset, which is obtained with different combination of parameters, contains a six-tuple of signal features (T_m, P_m, B_m,. T_std, P_std, B_std). The standard deviation is proportional to the uncontrolled process changes, whereas the mean value is correlated with the amount of energy of the radiation emitted. The script was then readapted to all tests carried out in the experimental campaign, the results of which were then compared.

Results and Discussion

With the aim of developing better in-process monitoring, this paper focuses on finding correlations between the data detected by the monitoring system with the typical welding process characteristics.

Welding characterization

From a first rough analysis of the weld's micrographs, it is clear that the process parameters utilized result in a wide range of outcomes, from unsuccessful joining to full cutting of the specimen. A high-quality weld should not have variations in the weld profile and the weld penetration depth should be such as to ensure the connection without leading to overpenetration: excessive weld penetration depth raises the possibility of damaging nearby components (such as electrodes), leading to future gas leaks that might cause a thermal runway.

The micrographs reported in Fig. 2 point out the different characteristics of the weld bead morphology of Al-Cu and Cu-Al configurations when a
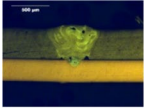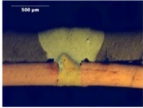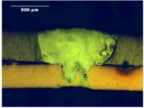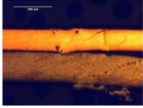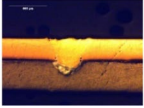

P[W]	900	1200	1500	1800
Al-Cu				-
Weld Width [µm]	687	868	1054	-
Cu-Al	-			
Weld Width [µm]	-	170	495	590

Fig. 2 Corresponding micrographs and weld bead width taken at the middle of trace when the *multimode* source is exploited at 200 mm/s speed

multimode source is exploited. The following considerations are valid for single source tests also. When the laser beam interacts with aluminum first, its weld bead tends to be larger at the top and narrower at the bottom. While if the first interaction is with the copper, the situation is the opposite. The Table 3 showing the weld dimensions performed with various parameters illustrates the previously mentioned trend. This behavior is due to the different physical properties of the two metals involved in the process, in terms of heat conduction coefficient and melting temperature (see Table 1). When the aluminum is at the top side, the laser beam melts, at first, the material that has the lower temperature melting point and then the copper that is situated at the interface between the two sheets. Copper has a much higher melting point and a higher thermal conductivity than aluminum, that's why it melts to a much lower extent.

When copper is at the top side, heat is transferred very quickly at the interface with aluminum which, because of the lower melting temperature, melts abruptly and, if the energy is excessive, tends to favor a complete penetration of the specimen [19].

From Table 4 it can be stated that it is generally true that the multimode weld lengths are larger than the single mode ones. As the power is raised, the width of the weld likewise grows.

The higher thermal conductivity and melting point of copper, together with the larger spot size, have resulted in the need for higher specific energies to melt the copper layer: a complete penetration of the weld is reached at 1800W when a multimode source is used, while 1000 W for the single mode.

From the observation of the sample morphology of both configurations, two opposed types of defects are emphasized when the maximum and lowest energy densities are applied. Figure 3 shows that if the material receives either too much or too little energy, there are two possible defects. In the first case, the excessive energy leads the melt pool of the keyhole to be unstable and to have tumultuous motions with the formation of bubbles and intermetallics which make the joint brittle. In contrast, the joint is not formed if the material does not absorb enough energy.

Table 3 Process parameters investigated

			Power [W]	Speed [mm/s]	Weld length [mm]
Multi mode	Test 1	Al-Cu	900–1200-1500	100–200-300	48
		Cu-Al	1200–1500-1800	100–200-300	48
Single mode	Test 2	Al-Cu	800–1000-1200	120–240-360–480	48
		Cu-Al	800–1000-1200	200–300-400–500	48
	Test 3	Al-Cu	800–1000-1200	120–240-360–480	100
		Cu-Al	800–1000-1200	200–300-400–500	100

Table 4 Multimode and single mode weld length

MULTIMODE									
Al—Cu	P[W]				**Cu—Al**	P[W]			
	900	1200	1500	200 [mm/s]		1200	1500	1800	200 [mm/s]
Weld length [μm]	685	870	990		Weld length [μm]	170	595	500	
Interface length [μm]	180	315	470		Interface length [μm]	145	330	415	
Depth penetration [μm]	85	300	300		Depth penetration [μm]	25	50	400	
Aspect ratio [μm]	0,12	0,35	0,30		Aspect ratio [μm]	0,15	0,08	0,80	
SINGLE MODE									
Al—Cu	P[W]				**Cu—Al**	P[W]			
	800	1000	1200	240 [mm/s]		800	1000	1200	200 [mm/s]
Weld length [μm]	700	670	595		Weld length [μm]	315	420	320	
Interface length [μm]	220	300	190		Interface length [μm]	0	250	260	
Depth penetration [μm]	145	300	300		Depth penetration [μm]	0	300	300	
Aspect ratio [μm]	0,21	0,45	0,51		Aspect ratio [μm]	0,00	0,71	0,93	
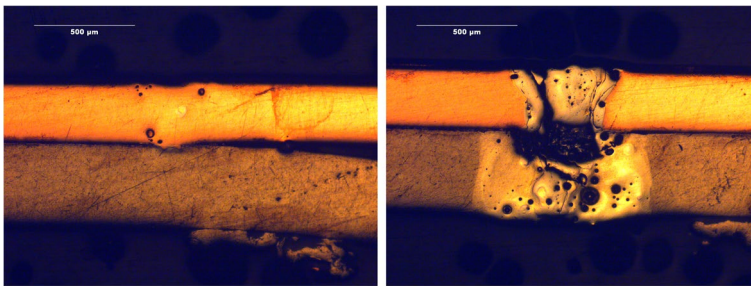
Fig. 3 Cross sections of Cu-Al samples when the lowest and excessive energy density is applied

Plasma and Temperature

In the first place, the welds performed with the multimode fiber source were initially analyzed and the results of test 1 were compared with each other. Al-Cu configuration was analyzed in the first place. PS and TS monitored during the laser welding process are reported in Fig. 4. If speed is fixed (v = 100 mm/s), there is a linear correspondence between the two signals and power: if power steps up from 900W (blue line) to 1500W (yellow line), PS and TS increase also. It can be noticed that the trend of PS along the trace over time mirrors that of the temperature: a

Fig. 4 A)Plasma and **b**) Temperature vs time as power ranges from 900 to 1500W for fixed velocity of 100 mm/s. Current data refers to Al-Cu configuration
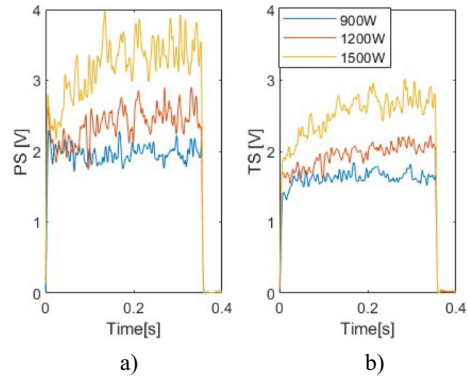

progressively increasing value can be noticed, which gets steeper as the laser power applied grows. For example, the increase of PS along the trace changes from 3.24% for lower power to 28% for 1500W.

This similarity between the two signals can be related to the fact that the temperature measured on the surface directly affects aluminum's vaporization and its alloy elements leading to the opening or closing of the keyhole. This observation agrees with the findings of Franciosa [6] and Eriksson et al. [22] who state that temperature and plasma signals are strongly correlated with Pearson's correlation coefficient above 94%. This suggests that the plasma plume emits not only in the UV/visible spectrum but also contributes to thermal radiation in the IR, it is therefore necessary to remove the PS from the TS.

The graph in Fig. 5 describes the effect of *speed* on the process: within the process parameters window analyzed, the trend of the signals becomes more stable (less oscillating) for high-speed values up to assuming an almost constant trend (like for v = 300 mm/s). This effect is more evident for higher power (1500W), as it is highlighted in Fig. 5 by the yellow squares. From a process point of view, this data behavior could be explained as follows: for low speeds, during the laser-aluminum interaction, the component increases its temperature moment by moment since not all the heat can be dissipated by conduction. Therefore, it is logical to think that, by heating continuously, the characteristics

Fig. 5 Influence of speed on the welding process in test 1: for higher values of speed which ranges from **a**) 100 mm/s **b**) 200 mm/s to **c**) 300 mm/s, the standard deviation of the signal decreases
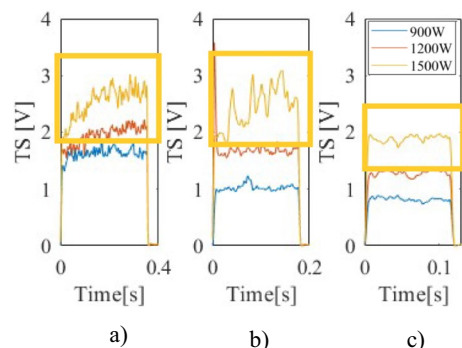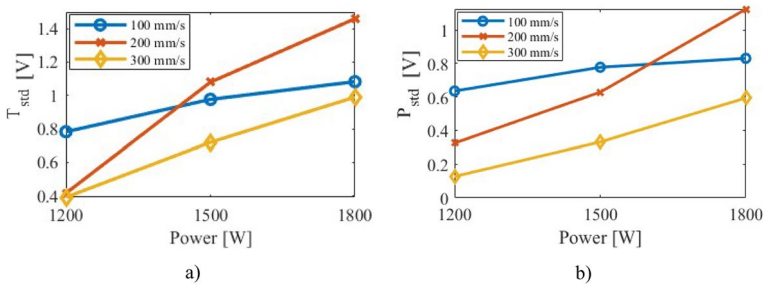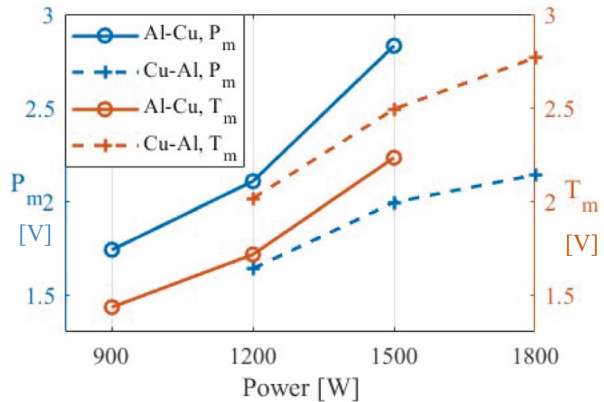
Fig. 6 A) Temperature and **b**) Plasma signals standard deviation for test 1 Cu-Al. As laser power increases and speed is diminished, an increasing trend can be noticed, leading to keyhole instability

Fig. 7 Mean values of PS [V] when a multimode source is exploited and speed is fixed at 200 mm/s for both Al-Cu and Cu-Al configurations

of the joint vary from the beginning to the end of the weld bead. This problem of heat accumulation during welding is emphasized for low speeds that lead to a longer interaction time and the amount of heat absorbed by the material increases with it. In the graphs in Fig. 5 this behavior is very evident: as the speed increases from 100 mm/s (a) to 300 mm/s (c) the signals are much less oscillating and more centered on the average value, which, presumably, is equivalent to a more homogeneous, sound weld bead along the track. To sum up, BS and TS standard deviation (T_{std}, P_{std}) increases as laser power increases and decreases for higher speeds, which comes to a higher energy density on the material. This feature is found to be more relevant for the Cu-Al configuration, hence the Fig. 6 is reported. This means that the more energy density is applied, the more the signal oscillates, hence the more unstable the keyhole gets. As previously anticipated, the mean value and the standard deviation of PS and TS were calculated for every test over the entire measurement signal of the weld.

The increasing linear relationship is consistent not only for T_{std} and P_{std}, but also for PS. The average between the two repetitions gives the final values P_ m and T_ m. The resulting values are plotted in Fig. 7 when a multimode laser source was exploited. Both Al-Cu and Cu-Al configuration values are reported.

There is clear evidence of a linear relationship between power and monitoring signals. A similar trend was identified also for weld-bead width. Overpenetration is esteemed from 1200 W, thus a mean value of PS and TS should stay below 2 V, according to Fig. 7. The same graph has been made for the single mode, but P_m and T_m values are so small (under 1 V) that is hard to state which is the optimal value for a good-quality weld.

Another thing that can be noticed is that the average amount of metallic vapor produced during the interaction between the laser beam and the aluminum is way higher than that found for welding the copper first: in Fig. 7 Al-Cu P_m curve assumes plasma values ranging in an interval that is higher than the Cu-Al P_m. This happens because aluminum has a lower phase transition temperature than copper and therefore vaporizes before. The width variation can then be monitored by the signal values of either plasma or thermal radiation during welding.

It is consequently confirmed that the control of the laser power based on thermal radiation values can minimize the variation in the bead width.

In the section "welding characterization", the defective joints obtained for high and low energy densities were observed. When the materials absorb more energy, the photodiodes recorded a higher radiation intensity for signals TS, PS and a lower intensity for BS, as expected. By looking at the average values of the three signals acquired for three different energy values (maximum, minimum, and optimal), we are able to determine an ideal working window. Large energy density Es in the TS and PS signals exhibit a greater standard deviation, which denotes weaker weldability stability. (Fig. 8).

These results for the single mode tests were not as straightforward, this is why results are not reported.
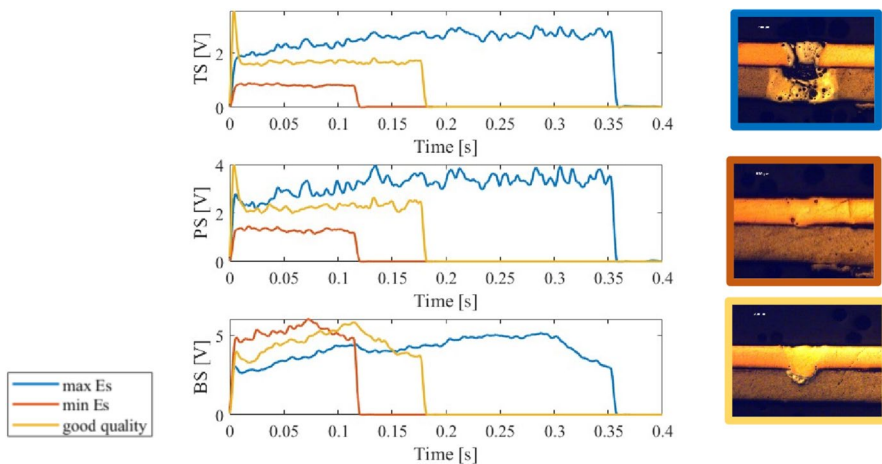

Fig. 8 Weld defects when either too much **a**) or too less **b**) energy is absorbed by the materials. Micrographs of Cu-Al configuration when a multimode laser source is exploited at max Es calculated at 1200 W 100 mm/s and min Es calculated at 1200 W and 200 mm/s

Back-Reflection

In the following paragraph BS is analyzed in test 1 Al-Cu. A comparison is then made with the data obtained in test 3 to comment the influence of the welding length. For tests 2 and 3 similar results were obtained, therefore the discussion can be extended for all Al-Cu tests. For the Cu-Al configuration such a marked trend was not evident: as the power and speed change, the signals mean values were almost steady, as Fig. 9 states. In general, it is well known that material absorptivity decreases with an increase in the welding speed [4]. As the welding speed increases, the molten pool becomes smaller, and the melt zone in front of the keyhole is also narrower (or thinner). That is, at higher welding speeds, a part of the laser beam is irradiated on the thin melt zone and solid metal surface; consequently, the laser back reflection increases, and the ratio of a laser beam absorbed into the keyhole decreases. The histogram in Fig. 9 testimony the latter consideration: increasing speed, the back reflection signal increases.

The BS itself is characterized by a fast peak near the central area followed by a fast drop, decreasing towards the end of the track. The bell-shaped pattern is probably due to the fact that the sensor, remaining integral with the laser head during the whole welding process (as a galvo head is expected to work), is able to collect all the radiations only in the configuration in which the laser head is positioned at the center of the trace and the beam is perpendicular to the surface. In all other welding positions, the inclination of the laser beam towards the surface increases and makes a good percentage of the light radiation going out from the sensor's reading range. For this reason, to make comparison analysis, the maximum value is considered, which is the peak point of the hilly trend. In support of this assumption, test 3 was carried out, where only the length of the track was changed. It was found that the bell-shaped trend is more marked: the sensor will receive very weak light radiation from the points furthest from the center of the weld bead because of the greater inclination. By making the weld bead longer, the surface temperature of the aluminum and the plasma detected decreases, if compared with the previous tests. (Fig. 10).

Looking at test 1, a comparison between BS collected during Al-Cu and Cu-Al configuration was carried out. It is clear that BS on copper is always greater because

Fig. 9 Peak values of the Back reflection-time signal at varying power and laser speed for test 1 Al-Cu. It can be noticed that as the speed increases also BS increases as a smaller amount of laser beam is absorbed because of the narrower weld bead formed
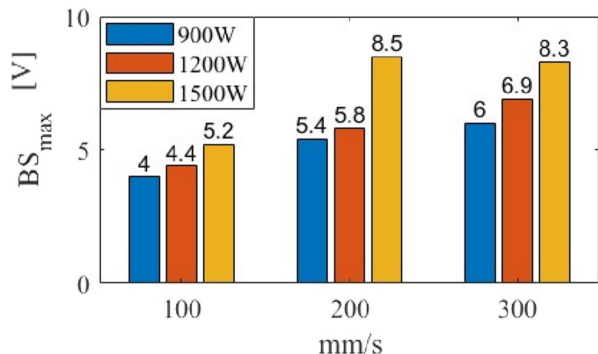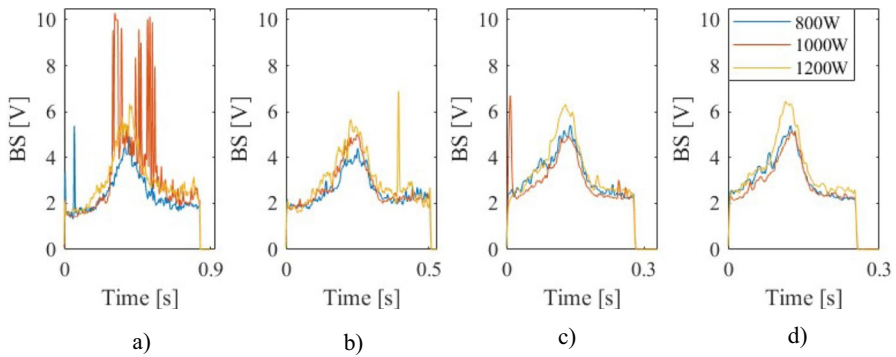
Fig. 10 Hilly trend of the BS-time at varying power and speed that ranges from a) 120 mm/s to d) 480 mm/s (on the right) for test 3. The bell-shaped trend in longer weld beads is more marked: the sensor will receive very weak light radiation from the points furthest from the center of the weld bead because of the greater inclination of the laser beam

it has a lower absorption coefficient than aluminum. Table 5. shows the percentage increase in the back reflection value B_m between the Al-Cu and Cu-Al configuration. B_m is the average between the two repetitions performed for test 1. The percentage increase formula that has been used is the following: (new value – old value) / old value *100%, where the new and old value refer, respectively, to B_m calculated for Cu-Al and Al-Cu configuration. Comparisons between all speeds (100 mm/s, 200 mm/s, 300 mm/s) and powers (900 W, 1200 W, 1500 W) parameters tested are also reported.

Table 5. Percentage increase values from Al-Cu to Cu-Al configuration in the operating window considered

	Speed [mm/s] →		
Power [W] ↓	106%	165%	170%
	65%	154%	133%
	133%	82%	96%

Statistical Analysis

In order to hold together the results from the whole experimental campaign, the spot dimension has to be taken into account as single and multimode sources were exploited. For every set of parameters, the mean value and the standard deviation were calculated for each weld bead and plotted against energy density.

As Fig. 12 states, TS can be modelled with a linear regression with good accuracy. In fact, the statistical analysis obtained with MATLAB shows a very low p-value

and an R^2 very close to unity ($R^2 = 90\%$), suggesting that the linear model used for temperature variable interpolates the data very well. However, this correlation is not true for back reflection and plasma variables, whose intensity depends on the laser source exploited for the experiment, as Fig. 13 and 14 point out. Hence, two different models must be implemented to describe the welding process carried out with two different sources. In order to monitor the stability of the process, the standard deviation of plasma (PS_{std}), temperature (TS_{std}) and back-reflection (B_{std}) versus Energy density Es were plotted. In this account, some considerations were raised: the TS_{std} graph in Fig. 11 a) shows clearly three patterns for both multi and single mode sources. These linear patterns were analyzed, especially for the multimode tests where it was more evident that the separate trends, with three points each, were characterized by equal speed. The histogram in Fig. 11 b) shows how the TS_{std}, which is directly correlated to process stability, depends more on power than speed: keeping the process at a constant speed, it becomes more instable as the power increases, and not vice versa. Consequently, it is possible to suggest changing the *power* as the variable input in the closed-loop system if any signal exceeds the threshold.

The same studies were made on Cu-Al configurations and the same results were observed.

Conclusions

This study clearly demonstrated that signal monitoring and control must be customized and readapted according to the spot of the laser beam and the material irradiated. Like the average amount of metal vapor produced during the interaction between the laser beam and *aluminum* is much higher than that detected for *copper* welding because aluminum has lower phase transition temperatures than copper and therefore vaporizes first. However, some considerations apply for all tests: power has
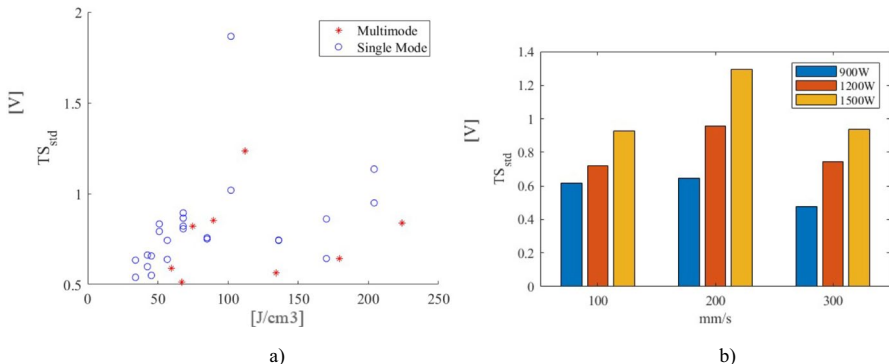

Fig. 11 A) TS_{std} against energy density Es for single and multimode sources. Three linear trends can be noticed with three scatter points each in every of which the speed is kept constant and the Power is increased. This consideration is validated by the histography in b) where for every speed, for an increased value of power, the process becomes more instable (standard deviation values increase)

proven to be the most influential parameter in every configuration of parameters, it could be then used as the feedback system's control variable. To sum up, the following results were obtained:

- The plasma trend mirrors that of the temperature: the temperature directly influences the vaporization of the aluminum and its alloying elements leading to the opening or closing of the keyhole. This suggests that the plasma plume emits not only in the UV/visible spectrum but also contributes to thermal radiation in the IR.
- There is an increasing linear relationship between plasma and power for the multimode source tests, a constant trend for the single mode ones. Observing the micrographs, the variation of the weld seam's width seems to follow the same tendency varying the power with the other parameters in play being equal.
- With the same power density as E_s the plasma values obtained in the multimode tests are greater than those obtained for the single mode tests for the Al-Cu configuration. This increased value is probably due to the greater width of the bead (the sensor detects more radiation).
- Within the window of process parameters analyzed, if high speeds were set, the trend of the signals stabilizes (less oscillating) until it assumes an almost constant trend. Hence, the standard deviation of the signal disclosed an explicit correlation with the stability of the process. This consideration is valid within the considered operative window. It is possible that the signal turns to be unstable if the speed is increased more.
- The back-reflection varies with a bell-shaped trend: the sensor is able to detect all radiations only in the configuration in which the laser head is located in the center of the trace and the light beam is perpendicular to the surface. In all other positions, a good percentage of the light radiation goes out of the reading range of the sensor. This behavior only affects the signals but not the weld quality itself.
- Windows of good weldability can be identified by comparing the cross-section's quality with the related signals.

Future work

Based on these observations, future technological implementations might follow:

It is conceptually possible to exploit plasma as an input to regulate the power with feedback control to keep the temperatures constant during the process.

If the consideration that was made on the back-reflection signal is true, it therefore makes this signal of little use for the analysis of the single trace but can only be evaluated in a comparative way with a pre-acquired signal on a bead, whose properties are considered acceptable.

The takeaway from the comparison between Al-Cu and Cu-Al configurations is that any threshold value for the bead control strictly depends on the first material irradiated.

During the analysis of the dataset, the width of the bead emerged to be a relevant parameter for the control of the opening/closing of the keyhole. This observation led us to consider the implementation of a camera system on the laser head capable of measuring the variations in shape and size of the keyhole as a possible evolution of this research. In this way, the correlation between the data detected by the sensors and the welding behavior observed by the high-speed imaging shall provide greater precision in welding control, guaranteeing the required quality. It is essential to have a larger dataset available in order to apply Machine Learning and Artificial Intelligence techniques to be able to link the behavior of one or more sensors and match it to a specific real defect and ultimately, prevent it through feedback control. That is to say, humanizing the whole laser welding monitoring process (acquiring signals, analyze them and making monitoring targets) [9].

Appendix

Al – Cu

The following Figure shows the output of the linear regression returned by Matlab with the corresponding R^2 and p-value. The p-value of the variable Es is very low 4.59e-17, which means that it is statistically significant in the model.

The R^2 is equal to 90%. It can therefore be stated that the linear model applied interpolates the data well. The linear regression model is the following: $T_m = -0.022436 + 0.0086192$ Es.

This graph highlights that for higher Es values the average temperature values are more spread out than those for low energy densities.

Fig. 12 Linear regression for TS Al-Cu with a $R^2 = 90\%$
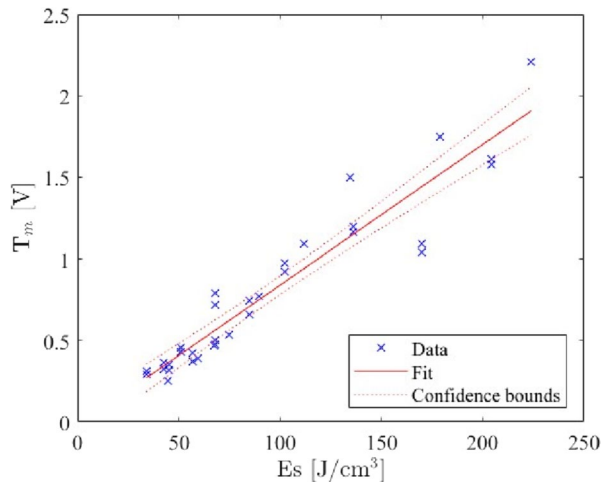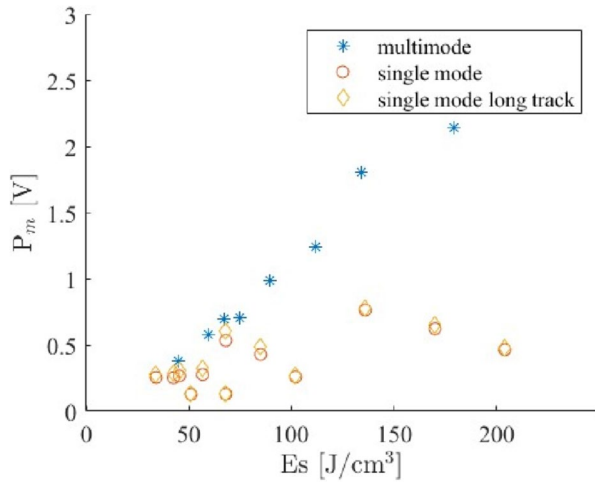
Fig. 13 Plasma values for both single mode and multimode sources

The average plasma signals of the two repetition P_m was calculated for every test and plotted against energy density Es. If a multimode source is exploited, the intensity of plasma radiation recorded grows with power density (E_s). On the other hand, if a single source is exploited, the variation of P_m against Es is not significant.

Unlike copper, aluminum seems to have a back reflection that increases with power: each source is split into three groups (three speeds) of three points each, representing the increase in power. As seen in Fig. 16, B_m on copper remains constant while Es varies. Furthermore, if copper is irradiated first, in the multimode case, B_m has higher values than for a single mode with the same Es. If Aluminum is

Fig. 14 B_m values plotted against energy density Es for Al-Cu configuration

a)   b)
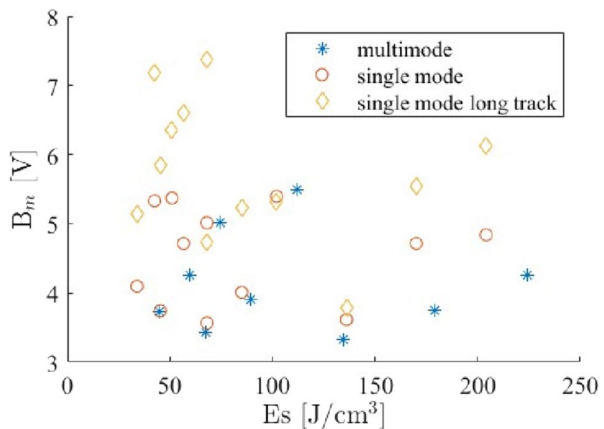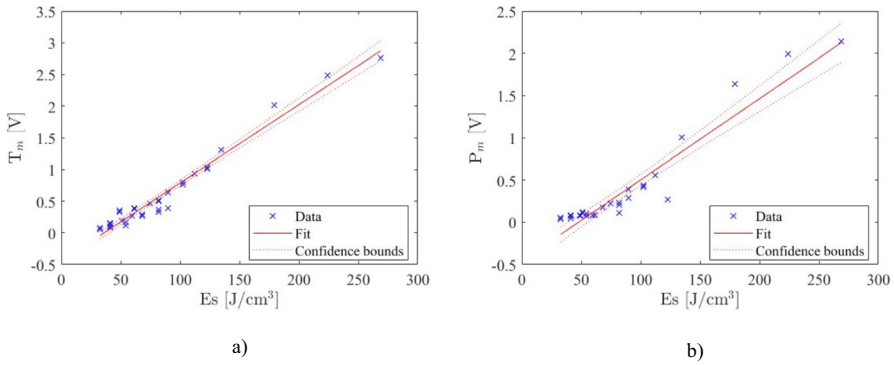
Fig. 15 Linear regression for TS and PS Cu-Al with a $R^2 = 97\%$ and $R^2 = 90\%$ respectively

at the top, this claim is untrue: B_m values remain pretty much alike, as Fig. 14 states. The length of the weld track is shown in this graph as yellow diamond dots.

Figures 15 a) and b) show the output of the linear regression returned by Matlab of T_m and P_m.

Both p-values of the variable Es shown in Table 5. are very low.

The R^2 are close to unity, hence the linear model interpolates the data very well.

Figure 16 plots B_m values plotted against Es when copper is irradiated first. It is evident that the Multimode source has a way higher Back reflection than the single mode. It is very clear also that Es is not a very much influent parameter when a single mode source is exploited since the scatter points are at the same level when Es changes.

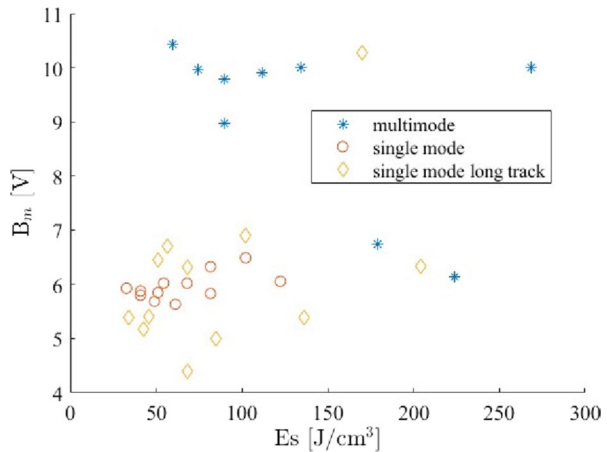**Fig. 16** B_m values plotted against energy density Es for Cu-Al configuration

Table 6. Estimated coefficients for T_m and P_m linear regression

Cu—Al	
Linear regression model	$T_m = -0.44845 + 0.0123 \, Es$
R-squared	0.968
p-value	7.84e-25
Cu—Al	
Linear regression model	$P_m = -0.45964 + 0.0096151 \, Es$
R-squared	0.894
p-value	1.12e-16

Data Availability The datasets generated during and/or analyzed during the current study are available from the corresponding author on reasonable request.

Declarations

References

1. Deal confirms zero-emissions target for new cars and vans in 2035, "https://www.europarl.europa.eu/news/en/press-room/20221024IPR45734/deal-confirms-zero-emissions-target-for-new-cars-and-vans-in-2035," [Online]
2. Ascari, A., Fortunato, A.: Laser dissimilar welding of highly reflective materials for E-Mobility applications. In: Joining Processes for Dissimilar and Advanced Materials. pp. 579–645. Elsevier (2022)
3. Wunderling, C., Bernauer, C., Geiger, C., Goetz, K., Grabmann, S., Hille, L., Hofer, A., Kick, M.K., Kriegler, J., Mayr, L., Schmoeller, M., Stadter, C., Tomcic, L., Weiss, T., Zapata, A., Zaeh, M.F.: Solutions of laser material processing for electric mobility – evaluation of the Technology Readiness Level.
4. Katayama, S.: Fundamentals and Details of Laser Welding. Springer Singapore, Singapore (2020)

5. Kogel-Hollacher, M.: The full potential of photonics in e-mobility: an overview. The Laser User Magazine. (2020)
6. Chianese, G., Franciosa, P., Nolte, J., Ceglarek, D., Patalano, S.: Characterization of Photodiodes for Detection of Variations in Part-to-Part Gap and Weld Penetration Depth During Remote Laser Welding of Copper-to-Steel Battery Tab Connectors. J. Manuf. Sci. Eng. **144**, 071004 (2022). https://doi.org/10.1115/1.4052725
7. Purtonen, T., Kalliosaari, A., Salminen, A.: Monitoring and Adaptive Control of Laser Processes. Phys. Procedia **56**, 1218–1231 (2014). https://doi.org/10.1016/j.phpro.2014.08.038
8. You, D.Y., Gao, X.D., Katayama, S.: Review of laser welding monitoring. Sci. Technol. Weld. Joining **19**, 181–201 (2014). https://doi.org/10.1179/1362171813Y.0000000180
9. Cai, W., Wang, J., Jiang, P., Cao, L., Mi, G., Zhou, Q.: Application of sensing techniques and artificial intelligence-based methods to laser welding real-time monitoring: A critical review of recent literature. J. Manuf. Syst. **57**, 1–18 (2020). https://doi.org/10.1016/j.jmsy.2020.07.021
10. Will, T., Schwarzkopf, K., Hölbling, C., Müller, L., Schmidt, M.: Feature extraction based on scalable hypothesis tests from photodiode data in laser welding processes. Procedia CIRP. **111**, 527–531 (2022). https://doi.org/10.1016/j.procir.2022.08.084
11. Lee, K., Kang, S., Kang, M., Yi, S., Kim, C.: Estimation of Al/Cu laser weld penetration in photodiode signals using deep neural network classification. J. Laser App. **33**, 042009 (2021). https://doi.org/10.2351/7.0000506
12. Blug, A., Carl, D., Höfler, H., Abt, F., Heider, A., Weber, R., Nicolosi, L., Tetzlaff, R.: Closed-loop Control of Laser Power using the Full Penetration Hole Image Feature in Aluminum Welding Processes. Phys. Procedia **12**, 720–729 (2011). https://doi.org/10.1016/j.phpro.2011.03.090
13. Sokolov, M., Franciosa, P., Sun, T., Ceglarek, D., Dimatteo, V., Ascari, A., Fortunato, A., Nagel, F.: Applying optical coherence tomography for weld depth monitoring in remote laser welding of automotive battery tab connectors. J. Laser App. **33**, 012028 (2021). https://doi.org/10.2351/7.0000336
14. Franciosa, P., Sokolov, M., Sinha, S., Sun, T., Ceglarek, D.: Deep learning enhanced digital twin for Closed-Loop In-Process quality improvement. CIRP Ann. **69**, 369–372 (2020). https://doi.org/10.1016/j.cirp.2020.04.110
15. Kim, H., Nam, K., Oh, S., Ki, H.: Deep-learning-based real-time monitoring of full-penetration laser keyhole welding by using the synchronized coaxial observation method. J. Manuf. Process. **68**, 1018–1030 (2021). https://doi.org/10.1016/j.jmapro.2021.06.029
16. Franciosa, P., Sun, T., Ceglarek, D., Gerbino, S., Lanzotti, A.: Multi-wave light technology enabling closed-loop in-process quality control for automotive battery assembly with remote laser welding. In: Negahdaripour, S., Stella, E., Ceglarek, D., and Möller, C. (eds.) Multimodal Sensing: Technologies and Applications. p. 9. SPIE, Munich, Germany (2019)
17. Seibold, M., Friedmann, H., Schricker, K., Bergmann, J.P.: Process control by real-time pulse shaping in laser beam welding of different material combinations. Procedia CIRP. **94**, 769–774 (2020). https://doi.org/10.1016/j.procir.2020.09.137
18. Dimatteo, V., Ascari, A., Fortunato, A.: Continuous laser welding with spatial beam oscillation of dissimilar thin sheet materials (Al-Cu and Cu-Al): Process optimization and characterization. J. Manuf. Process. **44**, 158–165 (2019). https://doi.org/10.1016/j.jmapro.2019.06.002
19. Fortunato, A., Ascari, A.: Laser Welding of Thin Copper and Aluminum Sheets: Feasibility and Challenges in Continuous-Wave Welding of Dissimilar Metals. Lasers Manuf. Mater. Process. **6**, 136–157 (2019). https://doi.org/10.1007/s40516-019-00085-z
20. Precitec: LWM Expert Training Book.
21. Andreev, A.: Smart Laser Welding Heads Provide Excellent Quality: Concerted Functionality enables High Productivity and efficiency. LTJ. **6**, 20–22 (2009). https://doi.org/10.1002/latj.200990068
22. Eriksson, I., Powell, J., Kaplan, A.F.H.: Signal overlap in the monitoring of laser welding. Meas. Sci. Technol. **21**, 105705 (2010). https://doi.org/10.1088/0957-0233/21/10/105705
23. Olsson, R., Eriksson, I., Powell, J., Kaplan, A.F.H.: Advances in pulsed laser weld monitoring by the statistical analysis of reflected light. Opt. Lasers Eng. **49**, 1352–1359 (2011). https://doi.org/10.1016/j.optlaseng.2011.05.010

Publisher's Note Springer Nature remains neutral with regard to jurisdictional claims in published maps and institutional affiliations.